

Title: A Phase 0 Trial of Ceritinib in Patients with Brain Metastases and Recurrent Glioblastoma

Shwetal Mehta¹, Roberto Fiorelli¹, Xun Bao², Chelsea Pennington-Krygier¹, Alanna Derogatis¹, Seongho Kim², Wonsuk Yoo¹, Jing Li² and Nader Sanai¹

Affiliations: ¹Ivy Brain Tumor Center, Barrow Neurological Institute, Phoenix, AZ 85013
²Karmanos Cancer Institute, Wayne State University School of Medicine, Detroit, MI 48201

Corresponding Author: Nader Sanai, MD, FAANS, FACS
J.N. Harber Professor of Neurological Surgery
Director, Division of Neurosurgical Oncology
Director, Ivy Brain Tumor Center
Barrow Neurological Institute
Phoenix, Arizona
Email: Nader.Sanai@ivybraintumorcenter.org
Phone: (602) 406-8889

Key Words: Phase 0, Ceritinib, brain metastases, glioma, ALK, IGFR1, FAK

Running Title: Phase 0 Study of Ceritinib in Brain Tumors

Word Count in Abstract: 247

Word Count in Text: 4124

No. of References: 32

No. of Tables/Figures: 6

Conflicts: The authors declare no potential conflicts of interest

Funding: Novartis Pharmaceuticals
The Ben & Catherine Ivy Foundation

Statement of Translational Relevance:

Overactivation of tyrosine kinase pathways plays a key role in driving brain tumor proliferation. Ceritinib is an orally available, potent inhibitor of anaplastic lymphoma kinase (ALK), insulin growth factor 1-receptor (IGF1R), and focal adhesion kinase (FAK). To provide the first comprehensive analysis of ceritinib's CNS tumor penetration profile, we completed a Phase 0 clinical trial in preoperative patients with brain metastasis or recurrent glioblastoma. Ceritinib is highly bound to plasma proteins and brain tumor tissues and its unbound drug concentrations in brain tumor tissue appear not to be sufficient for target inhibition of pFAK, pIGF1R, and pIRS1.

Abstract

Background: Ceritinib is an orally bioavailable, small molecule inhibitor for ALK/IGFR1/FAK, which are highly expressed in glioblastoma and many brain metastases. Preclinical and clinical studies indicate that ceritinib has anti-tumor activity in central nervous system (CNS) malignancies. This Phase 0 trial measured the tumor pharmacokinetics (PK) and tumor pharmacodynamics (PD) of ceritinib in patients with brain metastasis or recurrent glioblastoma.

Methods: Preoperative brain tumor patients with tumors demonstrating high expression of pSTAT5b/pFAK/pIGFR1 were administered ceritinib for 10 days prior to tumor resection. Plasma, tumor, and cerebrospinal fluid (CSF) samples were collected at predefined timepoints following the final dose. Total and unbound drug concentrations were determined using LC-MS/MS. In treated tumor and matched archival tissues, tumor PD was quantified through immunohistochemical analysis of pALK, pSTAT5b, pFAK, pIGFR1, and pIRS1.

Results: Ten patients (3 brain metastasis, 7 glioblastoma) were enrolled and no dose-limiting toxicities were observed. Ceritinib was highly bound to human plasma protein (median fraction unbound (F_u), 1.4%) and to brain tumor tissue (median F_u , 0.051% and 0.045% in Gadolinium-enhancing and -nonenhancing regions respectively). Median unbound concentrations in enhancing and nonenhancing tumor were 0.048 and 0.006 $\mu\text{mol/L}$, respectively. Median unbound tumor-to-plasma ratios were 2.86 and 0.33 in enhancing and nonenhancing tumor, respectively. No changes in pharmacodynamic biomarkers were observed in the treated tumor samples as compared to matched archival tumor tissue.

Conclusion: Ceritinib is highly bound to plasma proteins and tumor tissues. Unbound drug concentrations achieved in brain metastases and recurrent glioblastoma patients were insufficient for target modulation.

Introduction

The prognosis for patients with non-benign primary or secondary brain tumors is dismal. In metastatic brain disease, the most frequent tumors of origin are lung (36-64%), breast (15-25%), and skin (5-20%) (1). Metastatic brain tumor treatment typically involves repeated cycles of surgery plus radiotherapy, but is often incurable. Among primary brain tumors, glioblastoma is the most common and the most lethal, with a median survival of 16 months despite repeated cycles of surgery, radiotherapy, and chemotherapy. Effective, brain-penetrant adjuvant therapies are in short supply for both primary and secondary brain tumor patients.

The blood-brain barrier (BBB) is a perennial problem for developing such new therapies(2) and, alongside the lack of targetable driver mutations, ranks among the most formidable obstacles to brain tumor drug discovery. The BBB is a protective lining that surrounds capillaries in the brain parenchyma and tightly controls the ingress of substances into the brain from the circulation. Although it is heterogeneous in its permeability and modestly compromised in the setting of an intracranial tumor, the net effect of the blood-brain barrier is that it excludes most anticancer agents from the tumor, contributing to the poor performance of many new drugs.

Targeted drugs are only effective when directly inhibiting strong disease drivers, yet only a small fraction of brain tumors feature known, actionable drivers. In this regard, multi-targeted agents may be advantageous using a polypharmacology approach(3). Ceritinib is a second-generation, selective inhibitor of receptor tyrosine kinases (RTK) Anaplastic Lymphoma Kinase (ALK), Insulin Growth Factor 1 Receptor (IGF1R), and Focal Adhesion Kinase (FAK). It is FDA-approved for treatment of the 5% of non-small cell lung cancer (NSCLC) patients with tumors harboring a gene rearrangement between echinoderm microtubule-associated protein like 4 and anaplastic lymphoma kinase (EML4-ALK) and who have failed crizotinib(4-7). The efficacy of ceritinib in crizotinib-resistant ALK(+) NSCLC tumors has been attributed to inhibition of IGF1R in addition to ALK signaling, since activation of IGF1R is an identified mechanism of resistance against ALK-inhibitors(8).

Insulin-like Growth Factor 1 Receptor (IGF1R) is an RTK that belongs to the insulin receptor family of kinases and promotes cancer cell proliferation and metastasis (9). In the CNS, IGF1R and its ligands (IGF1, IGF2 and insulin) not only play an important role during brain development, but are also implicated in brain tumor growth (10). IGF1R is overexpressed in both glioblastoma and several CNS metastases and is implicated in tumor progression (11,12). Ligand binding activates IGF1R through autophosphorylation and results in recruitment and phosphorylation of adaptor protein insulin receptor

substrate 1 (IRS1) (9). Phosphorylated IRS1 then triggers downstream mitogenic signaling through the PI3K/mTOR pathway. Several small-molecule inhibitors and antibodies have been tested to block IGF1R signaling in cancer, although none have demonstrated clinical efficacy(13).

Yet another target of ceritinib is focal adhesion kinase (FAK)(3), which regulates expression of IRS1 (downstream target of IGF1R) and also activates PI3K pathway (14-16). Activation of both IGF1R and FAK results in phosphorylation of IRS1 which in turn promotes tumor proliferation through AKT/mTOR pathway. Importantly, IGF1R and FAK overexpression and activation are widespread in both CNS metastases and glioblastoma, raising the possibility of a role for ceritinib as an adjuvant therapy targeting IGF1R(+) or pFAK(+) brain tumors (3,5,11,13,15,17). The roles of these aberrant pathways as oncogenic drivers of these tumors remain unknown.

Ceritinib is associated with the control of intracranial disease in ALK(+) NSCLC patients although, to date, no study has directly measured ceritinib drug concentrations in human tumor tissue. Of the 124 patients with brain metastases reported in the Phase 1 ASCEND-1 trial, 94 (n=19 ALKi-naïve and n=75 ALKi-pretreated) were included in a retrospective analysis. The intracranial disease control rate was 78.9% (15/19; 95% CI 54.4-93.9) in ALKi-naïve patients and 65.3% (49/75; 95% CI 53.5-76.0) in ALKi-pretreated patients. Of the 94 patients included in the retrospective study, 11 had measurable brain lesions with no prior brain irradiation and 6 achieved a partial intracranial response (18). More recently, ASCEND-7 was a Phase 2 study that evaluated the efficacy of ceritinib in ALK(+) NSCLC brain metastases and/or leptomeningeal disease (LMD) (19,20). Radiographic evidence of extracranial and intracranial response were detected across four treatment arms following ceritinib therapy (20,21).

Phase 0 clinical trials are commonly defined as first-in-human studies with no therapeutic or diagnostic intent, a limited number of patients, and micro-dosing of the experimental agent (22,23). These characteristics, however, are not essential for Phase 0 studies(24), which were introduced as a means of identifying pharmacokinetic and pharmacodynamic features of a tumor in response to novel therapy. For brain tumor patients, traditional Phase 0 design elements must be adjusted to accommodate the blood-brain barrier (BBB) and the significant risks of tumor tissue acquisition (25). In the reported study, we adapt the Phase 0 strategy (26,27) through subtherapeutic presurgical dosing instead of microdosing and through matched archival controls instead of pre- and post-treatment biopsies to assess pharmacodynamic effects. The study objectives were (1) to quantify the pharmacokinetic profile of unbound ceritinib within brain tumor tissue and (2) to identify the downstream molecular effects of ceritinib in patients with brain metastasis or recurrent glioblastoma.

Patients and Methods

This open-label, nonrandomized Phase 0 clinical trial (NCT02605746) was conducted by the Ivy Brain Tumor Center at the Barrow Neurological Institute in Phoenix, Arizona. The study was approved by our local institutional review board and conducted in accordance with the principles of the Declaration of Helsinki and the Good Clinical Practice guidelines of the International Conference on Harmonization. Written informed consent was obtained from all patients before screening.

Study population

All study patients were older than 18 years and presented with a brain metastasis or recurrent World Health Organization (WHO) IV glioma (i.e, glioblastoma) necessitating resection (Table 1). Using archival tissue from prior tumor resections, eligible brain metastases patients had tumors with pALK or IGF1R expression while glioblastoma patients had tumors positive for pFAK or IGF1R expression (minimum, >20% positive cells). Other inclusion criteria included an Eastern Cooperative Oncology Group (ECOG) performance status ≤ 2 , absolute neutrophil count (ANC) $\geq 1.5 \times 10^9/L$, hemoglobin (Hgb) $\geq 8g/dL$, Serum total bilirubin $\leq 1.5 \times$ upper limit of normal (ULN), aspartate transaminase (AST) $< 3.0 \times$ ULN, and alanine transaminase (ALT) $< 3.0 \times$ ULN. Patients who were febrile, had prior ceritinib treatment, were hypersensitive to any ceritinib excipients, had a history of disseminated bilateral fibrosis or interstitial lung disease, had a history of uncontrolled heart disease, had impaired GI function or disease, or were receiving strong inhibitors or inducers of CYP3A4/5 were excluded.

Study design

This study's primary objective was to determine the tumor concentration of unbound ceritinib following 10 oral doses of 750 mg in patients with brain metastases or glioblastoma. A secondary objective was to evaluate tumor PD biomarkers corresponding to ALK/IGF1R/FAK pathway activity. The 10-day interval was selected based upon estimates of duration to steady-state, as well as the number of days a preoperative brain tumor patient could safely delay a planned operation.

Enrolled Phase 0 patients were administered 750 mg/d (fasted) or 450 mg/d (with food) of ceritinib for 10 days prior to planned brain tumor resection. Patients were assigned to one of two time-escalation cohorts in which tumor resection was performed at either 4 or 24 hours following the final dose of ceritinib. During tumor resection, blood, cerebrospinal fluid (CSF), and tumor samples from Gadolinium-enhancing (brain metastasis and glioblastoma) and -nonenhancing (glioblastoma) regions (based on preoperative MRI and intraoperative neuronavigation) were collected for PK and PD analyses.

The first three study patients (all with brain metastases) were presurgically administered ceritinib 750mg PO QD under fasting. With the emergence of new data on the steady-state pharmacokinetics of ceritinib(4), this regimen was reduced to 450mg PO QD with food for all subsequent study patients (all with glioblastoma). The primary objective of the study protocol – tumor PK quantification – was not changed despite this modification. Patients were assigned to two time-escalation arms in which tumor resection was performed at 4 or 24 hours, respectively, following their final dose of ceritinib.

Statistical analysis

This is an exploratory study designed to evaluate a primary pharmacokinetic endpoint and secondary pharmacodynamic endpoints. No formal statistical hypothesis tests were performed and the sample size was justified based on feasibility. Descriptive statistics were performed to evaluate all tumor PK and PD measurements as well as patients' demographics and clinical characteristics. All continuous variables were summarized with means, standard deviations, coefficient of variation (CV) and ranges, and frequencies and proportions were used for all discrete data. In addition to these statistics, we calculated medians and geometric means due to the small samples and dependencies and exponential phenomena of pharmacokinetic parameters. Graphpad and SAS V9.4 were used to generate the data and plots.

Study clinical assessments

Adverse events were graded according to the Common Terminology Criteria for Adverse Events, version 4.03 (http://evs.nci.nih.gov/ftp1/CTCAE/CTCAE_4.03_2010-06-14_QuickReference_8.5x11.pdf). Demographic data and medical history were recorded for all study patients. Physical examination, vital signs, organ functions, and other safety assessments (Eastern Cooperative Oncology Group performance status, registration of concomitant medication, hematology, biochemistry, and urine analysis) were performed at baseline. Common Toxicity Criteria Adverse Event (CTC AE) 4.0 criteria were used to document adverse events.

Enrollment criteria

For brain metastases patients, samples from prior tumor resections were examined with immunohistochemistry staining for pSTAT5b and pJAK2, factors downstream of ALK signaling, as well as IGF1R staining. Immunohistochemistry staining for all samples was completed on the Leica Bond RX, a fully-automated platform using validated assays that were optimized with breast, lung, and melanoma tissue samples from the Biobank. Briefly, archival FFPE slides were stained with anti-pSTAT5b (Abcam,

#ab52211; 1:50), anti-pJAK2 (Abcam, #ab32101; 1:50), or anti-IGF1R (Cell Signaling, # 3027; 1:100) for assessing percentage of pSTAT5b(+), pJAK2(+), or IGF1R(+) cells.

For glioblastoma patients, samples from prior tumor resections were examined with immunohistochemistry staining for IGF1R and pFAK. Immunohistochemistry staining for all samples was completed on the Leica Bond RX, using validated assays that were standardized with archival glioblastoma tissue. Briefly, archival FFPE slides was stained with anti-IGF1R (Cell Signaling, # 3027; 1:100) and anti-pFAK pTyr397 (ThermoFisher, # 44-624G; 1:100) for assessing percentage of IGF1R(+) and pFAK(+) cells. Patients with tumor samples with >20% positive cells were deemed eligible for the trial. The stained slides were imaged using Aperio Versa System (Leica) and analyzed using ImageScope software. In parallel, the slides were also analyzed by a board-certified neuropathologist.

Pharmacokinetic evaluation

Blood pharmacokinetic samples were collected from each patient at pre-dosing, 0.5, 1, 2, 4, 6, 8 and 24 hours after the administration of the 9th presurgical dose of ceritinib. This day was chosen to avoid any confounding effects of brain surgery on day 10. Plasma was separated from whole blood by centrifugation (at 4°C, 1500 g for 10 minutes), and plasma samples were stored at -80°C until analysis. Surgical resection of tumors was performed at predefined time points following the administration of the 10th dose. Blood, tumor (including contrast-enhancing and nonenhancing regions for glioblastoma patients), and CSF samples were collected intraoperatively at 2-4, 6-8, or 23-25 h after the administration of the 10th dose. Tumor specimen locations were recorded with operating room MRI neuronavigation system, a standard surgical adjunct that registers preoperative MR imaging to the patients cranium. Each tumor sample was immediately rinsed with ice-cold PBS to remove residual blood, blot-dried, and snap frozen in liquid nitrogen.

The total concentrations of ceritinib in plasma, tumor, and CSF samples were determined using a validated liquid chromatography with tandem mass spectrometry (LC-MS/MS) method (28). The fraction unbound of ceritinib in plasma and tumor tissues were determined by equilibrium dialysis, and unbound drug concentration was calculated as the product of total concentration and fraction unbound (28).

Pharmacokinetic analysis

Plasma pharmacokinetic parameters for total and unbound ceritinib were estimated based on the observed plasma concentration time profiles using the non-compartmental analysis. These included the steady-state peak plasma concentration ($C_{ss,max}$), time to reach the $C_{ss,max}$ ($T_{ss,max}$), steady-state trough plasma

concentration ($C_{ss,min}$), steady-state area under the plasma concentration – time curve during one dosing interval (AUC_{τ}), apparent clearance for the total drug (CL/F), and unbound-to-total drug AUC ratio (AUC_u/AUC_t). The elimination rate constant (K) was estimated based on $C_{SS,min} = C_{SS,max} \times e^{-K\tau}$, where τ is dosing interval (24 h). The elimination half-life is estimated as $0.693/K$.

The extent of ceritinib penetration into the central nervous system (CNS) was assessed by the total drug tumor-to-plasma concentration ratio (K_p), unbound drug tumor-to-plasma concentration ratio ($K_{p,uu}$), and unbound drug CSF-to-plasma concentration ratio at the steady-state.

Pharmacodynamics analysis

To test the stability of proposed pharmacodynamic biomarkers in glioblastoma tissues (pFAK, IGF1R, pIGF1R, pIRS, cleaved caspase 3, Ki67), we analyzed a historical cohort of 4 matched primary and recurrent glioblastoma patients who received standard-of-care Stupp regimen and were not enrolled in the study. FFPE tissues were stained with anti-STAT5B (Abcam, #ab178941; 1:1000), anti-pSTAT5B (Abcam, #ab52211; 1:50), anti-pJAK2 (ab32101; 1:50), anti-FAK (Cell Signaling, #3285; 1:100), anti-pFAKTyr397 (ThermoFisher, #44-624G; 1:100), anti-IGF1R (Cell Signaling, # 3027; 1:100), anti-pIGF1R (Abcam, #ab39398; 1:50), anti-pIRS1 (ThermoFisher, #44-816G; 1:100), anti-histone H3 (Cell Signaling, #9701; 1:200), and cleaved caspase 3 (Cell Signaling, #9661; 1:300) using our standardized immunohistochemistry protocol with the BOND RX automated system (Leica Biosystems, Wetzlar, Germany). The stained slides were imaged and quantified using the Aperio Image analysis software (Leica Biosystems) to assess differences in positivity for the above antibodies. The slides and images were analyzed by a board-certified neuropathologist.

Pharmacodynamic assessment of the tumor tissue post-ceritinib treatment was conducted by comparing changes in biomarker levels in FFPE tissue from the patient's first tumor resection (at the time of initial diagnosis) and tumor tissue resected after presurgical drug exposure. To assess the pharmacodynamics effects of ceritinib in CNS metastases, phosphorylation of ALK, STAT5b and JAK2 were selected as primary determinants. For glioblastoma, we compared changes in IGF1R, FAK and IRS1 phosphorylation in pre- and post-ceritinib treated tissue. Other biomarkers assessed included the mitotic marker phosphohistone-3 and the apoptosis marker cleaved caspase-3. As a control, matched primary and recurrent glioblastoma tissues were used to assess changes in biomarker levels between primary and recurrent tumors.

Both archival FFPE tumor tissue and study specimens collected at the time of resection were assayed simultaneously using our standardized immunohistochemistry protocol with the Leica BOND RX automated system. For each run, we included positive (historical glioblastoma tissue) and negative controls (no primary antibody). Stained FFPE slides were imaged using a Leica DM55500 microscope and analyzed using Aperio Image analysis software.

Results

Patient population and safety

Three patients with brain metastases were accrued and their primary tumor sites were breast, head and neck and melanoma, respectively. Prior treatments for these patients included adriamycin and cyclophosphamide (4 cycles) plus taxol (1 cycle) and whole brain radiation for Patient 1 (breast); navelbine and cisplatin for Patient 2 (head and neck) and nivolumab and ipilimumab plus radiosurgery treatment for Patient 3 (melanoma). All patients had prior tumor specimens (from systemic disease sites) demonstrating IGF1R and/or ALK expression.

Seven recurrent glioblastoma patients were accrued, with all seven demonstrating WHO Grade IV histology and expression FAK. All glioblastoma patients had completed the Stupp regimen(29) prior to tumor recurrence and one glioblastoma patient had received a single treatment of bevacizumab 2 months prior to surgical resection. No glioblastoma patients received any other adjuvant chemotherapies or were treated with tumor-treating fields prior to enrollment.

Study patient demographics and clinical characteristics are described in Table 1. Three patients with CNS metastases received daily dose of 750 mg ceritinib, which is the maximally tolerated dose (MTD) (4), for 10 days prior to tumor resection. The subsequent seven recurrent glioblastoma patients received a daily dose of 450 mg ceritinib with low-fat diet which has been shown to lower the drug-associated GI toxicities and grade 3 or 4 adverse events (30). Presurgical ceritinib was well-tolerated and there were no dose-limiting toxicities. All observed toxicities at least possibly related to ceritinib were minor (CTCAE 4.0 grades 1 and 2), including diarrhea (20%), nausea (10%), vomiting (10%) and lymphopenia/thrombocytopenia (10%). All planned surgical resections occurred within the protocol-designated time interval following the last presurgical dose of ceritinib (median error, \pm 120 minutes). All ten evaluable study patients completed a 10-day course of ceritinib immediately prior to scheduled surgery.

Plasma and CNS pharmacokinetics

Table 2 summarizes the steady-state plasma pharmacokinetic parameters of total and unbound ceritinib in 10 patients. Following daily oral administration of ceritinib at 750 mg or 450 mg for 9 days, the geometric mean $C_{ss,max}$ of total and unbound ceritinib were 1.230 and 0.015 $\mu\text{mol/L}$, respectively; the geometric mean $C_{ss,min}$ of total and unbound ceritinib were 0.881 and 0.010 $\mu\text{mol/L}$, respectively. The fluctuation between steady-state peak and trough plasma concentrations of total ceritinib was 1.4-fold (geometric mean). The geometric mean elimination half-life ($T_{1/2}$) was estimated to be 60 h, and the geometric mean CL/F of total ceritinib was 41.2 L/h (range, 29.8 – 66.9 L/h) in 10 patients. Overall, the plasma pharmacokinetic parameters of ceritinib observed in our study were in line with those estimated from the population pharmacokinetics analysis involved a large cancer patient population (31).

Ceritinib was highly bound to human plasma proteins, with the median fraction unbound of 1.4% (range, 0.6% – 2.6%). The drug showed variable and extremely high binding to brain tumor tissues, with the median fraction unbound of 0.051% (range, 0.006% - 1.6%) and 0.045% (range, 0.006% - 0.21%) in enhancing and non-enhancing tumor regions, respectively (Table 3). The penetration of ceritinib into brain tumors and CSF was summarized in Table 3 and Figure 1. Across 2 to 24 h after the administration of the 10th dose, the median total ceritinib concentrations in enhanced and non-enhanced tumors were 36.10 nmol/g (or $\mu\text{mol/L}$) (range, 2.023 – 139.4) and 2.77 nmol/g (range, 1.259 – 36.35), respectively; whereas, the median unbound ceritinib concentrations in enhanced and non-enhanced tumors were 0.048 nmol/g (range, BLQ – 0.87) and 0.006 nmol/g (range, BLQ – 0.027), respectively, where BLQ is below the lower limit of quantitation. Ceritinib CSF concentrations (median, 0.012; range, 0.001 – 0.103 μM) were similar to unbound drug concentrations in non-enhancing tumor regions (Table 3 and Figure 1). The extent of CNS penetration is often assessed by K_p and $K_{p,uu}$, while $K_{p,uu}$ is more pharmacologically relevant. Ceritinib exhibited the median K_p of 33.14 (range, 2.49 – 95.86) and 3.49 (range, 1.55 – 37.14) in enhanced and non-enhanced tumors, respectively; whereas, it showed the median $K_{p,uu}$ of 2.86 (range, 0.01-40.6) and 0.33 (0.01-2.71) in enhanced and non-enhanced tumors, respectively. Notably, in one patient (Patient 1) with breast cancer brain metastasis, the ceritinib fraction unbound in the tumor was ~ 30-fold higher than the median value. As a result, the unbound ceritinib concentrations in both tumor and CSF were > 10-fold higher than the median levels of 10 patients and the K_p was unusually high (40.6) (Table 2).

Pharmacodynamic analyses

Among the three CNS metastases patients, PD analyses was performed on tissue samples from two patients (Patients 1 and 3; breast and melanoma) (Figure 2). Compared to the archival pre-treatment tissue from the primary tumor (breast and melanoma) the ceritinib-treated metastatic tissues had increased expression of pALK, pSTAT5b and pJAK2 and no significant difference in the mitotic marker pH3 and apoptosis marker cleaved caspase 3 (Figure 2). Among the 7 recurrent glioblastoma patients, one patient was excluded from PD analyses due to pseudoprogression evident in the acquired tissue (Patient 9). No significant changes in expression were observed in the tested biomarkers (pFAK, pIRS1, pIGF1R, cleaved caspase 3 and pH3) amongst the remaining 6 recurrent glioblastoma patient tumors after treatment with ceritinib (Figure 3).

Discussion

In this brain tumor Phase 0 study, we elucidate the pharmacokinetic and pharmacodynamic profile of ceritinib in plasma and tumor tissues of patients with CNS metastases and recurrent glioblastoma. These data represent the first ever analysis of ceritinib drug concentrations in human brain tumor tissue. Our findings indicate high binding of ceritinib to plasma proteins and brain tumor tissues and limited unbound drug exposure in the contrast enhancing and non-enhancing brain tumors.

Poor blood-brain penetration is a barrier to brain tumor drug development and adjuvant therapy efficacy (2). Although many nonrandomized studies of new CNS oncology agents use radiographic and clinical endpoints to assess drug effect, these efforts depend on preclinical and *in silico* analyses to predict the CNS penetrance of the agent. This approach has obvious limitations and can lead to assumptions of CNS penetrance that may confound assessments of clinical efficacy in metastatic disease, where brain tumor formation and progression is influenced by systemic disease status. In this study, we measure, for the first time, the brain tumor penetration and pharmacodynamic effects of ceritinib as it relates to the FAK and IGF1R signaling pathways in brain tumor patients. Our findings demonstrate that free drug levels are well below the biochemical IC50 of ceritinib for IGF1R and FAK (8nM and 30 nM, respectively) (3,32). Thus, ceritinib may not achieve pharmacologically-relevant drug concentrations in recurrent glioblastoma or select brain metastasis patients where these pathways are therapeutically-relevant.

Nevertheless, interindividual variability in ceritinib concentrations was observed among patients and, in a case of a breast cancer metastasis patient, resulted in significantly higher measured levels of unbound ceritinib. Drug non-specific binding to tissues is largely driven by non-specific binding to tissue phospholipids. The significantly lower binding of ceritinib in the breast cancer metastasis as compared to

glioblastoma may be due to different tissue compositions, especially in relative amounts of phospholipids. Further study with a larger sample size of patients with breast cancer brain metastasis is needed to confirm our observation and elucidate the underlying mechanism. Regardless, our data suggests that the limited unbound (i.e., pharmacologically active) drug exposure in studied brain tumors was mainly attributable to the high binding of ceritinib to plasma proteins and brain/tumor tissues.

The ASCEND-7 Phase 2 clinical trial in ALK(+) NSCLC patients with brain metastases assessed the intracranial effects of ceritinib using the modified RECIST v1.1 guideline. High disease control rate (DCR) was observed across all four arms of the study, which included prior radiation therapy (RT) and ALK inhibitor treatment (ALKi), no RT but prior ALKi, prior RT but no ALKi, and no prior RT or ALKi treatment. Patients in all four arms of this Phase 2 study had high overall response rate and DCR in extracranial disease. These data strongly suggest that ceritinib is CNS penetrant. Several differences between ASCEND-7 and this Phase 0 trial may explain the discrepancy between our observed low tumor drug concentrations and the clinical/radiographic responses reported in ASCEND-7: (1) unlike the patient population enrolled in ASCEND-7 study, none of the Phase 0 patients in this study were ALK(+) NSCLC. It remains possible that ALK(+) NSCLC is uniquely permeable to ceritinib, as compared to the brain tumor patients in this Phase 0 study. (2) BBB integrity is variable across different tumor types, owing to patient and tumor genetics, as well as the distinct cytoarchitectural features of each tumor type(33). This likely contributes to the interindividual variability observed in our study. (3) Additionally, although our protocol used enough presurgical ceritinib to reach steady-state, the total drug exposure was only 10 days, in contrast to the months-long regimen prescribed to ASCEND-7 patients.

Across all glioblastoma patients, we did not observe any PD effects on the downstream effectors of ALK, IGF1R and FAK based on pSTAT5, pJAK2, pIRS1 levels. There was also no significant change in proliferation or apoptosis markers in post-treatment samples. Lack of pharmacodynamic response could be attributed to the limited drug penetration, however, it is important to note that this PD analyses relied on control specimens from prior resections/biopsies (median interval, 12 months) that were not acquired immediately pre-treatment. Nevertheless, our data suggests that 10 days of ceritinib does not lead to target modulation, consistent with its observed limited CNS penetration. Further studies are warranted to better understand ceritinib's CNS penetration capabilities in the setting of other disease, including ALK(+) NSCLC brain metastases.

Phase 0, window-of-opportunity, and other tissue-based PK-/PD-driven clinical trial designs are starkly underrepresented in today's neuro-oncology and brain tumor drug development efforts. Over the past 50

years, only 22 such studies have been identified in the literature(25). Nevertheless, the value of such studies to guiding new therapeutic strategies for incurable brain tumors cannot be overstated. A positive result can provide the necessary justification to accelerate a drug's development. A negative result, such as in this study, sheds light on the limited potential of a new agent for CNS disease. Accordingly, our observations from this Phase 0 study of ceritinib indicate it should not be pursued as an anticancer agent in glioblastoma and select brain metastases due to its extremely limited penetration of these tumors. Collectively, this study underscores the utility of Phase 0 studies in precisely calculating brain tumor drug penetration, as well as in revealing the variability associated with tumor histologies in brain tumor patients. Our experience also serves as a reminder that brain tumor Phase 0 study results should be interpreted in context and not extrapolated beyond the tested circumstances.

Acknowledgements

We are grateful to the patients participating in this study. Results were presented at EANO 2019, ESMO Congress 2019 and SNO 2019.

Table 1. Patient demographics and clinical characteristics.

| Characteristics | N=10 |
|-------------------------------------|---------------|
| Sex (male/female) | 5/5 |
| Age (years) | 61 (40-72) |
| Weight (kg) | 175 (104-221) |
| Height (cm) | 69 (62-79) |
| ECOG/Zubrod Performance Status (n%) | |
| 0, n (%) | 3 (30%) |
| 1, n (%) | 5 (50%) |
| 2, n (%) | 2 (20%) |
| Diagnosis (n%) | |
| Brain metastases, n (%) | 3 (30%) |
| Glioblastoma, n (%) | 7 (70%) |
| Extent of Resection | |
| GTR, n (%) | 6 (60%) |
| STR, n (%) | 1, (10%) |
| Unknown, n (%) | 0 (0%) |
| Not applicable, n (%) | 3 (30%) |
| Prior Temozolomide, n (%) | 7 (70%) |
| Prior Radiotherapy (Y/N) | 10 (100%) |
| Prior Bevacizumab, n (%) | 1 (10%) |
| Timing of Ceritinib, n (%) | |
| At occurrence | 2 (20%) |
| First progression | 6 (60%) |
| Second progression | 2 (20%) |

Table 2. Steady-state plasma pharmacokinetic parameters of total and unbound ceritinib in patients.

| Total Ceritinib | | | | | | | | |
|--------------------------|-----------|-------------------------|------------------------------|-------------------------|------------------------------|-----------------------------|------------------------------------|----------------------|
| Patient# | Dose (mg) | T _{ss,max} (h) | C _{ss,max} (μmol/L) | T _{ss,min} (h) | C _{ss,min} (μmol/L) | AUC _τ (μmol/L·h) | CL/F (L/h) | T _{1/2} (h) |
| 1 | 750 | 8.1 | 2.234 | 24.0 | 2.096 | 45.052 | 29.8 | 260.3 |
| 2 | 750 | 6.0 | 1.230 | 24.0 | 0.766 | 20.097 | 66.9 | 35.2 |
| 3 | 750 | 6.0 | 1.834 | 24.1 | 0.920 | 24.633 | 54.6 | 24.2 |
| 5 | 450 | 7.9 | 1.020 | 21.6 | 0.935 | 19.748 | 40.8 | 172.0 |
| 7 | 450 | 4.4 | 1.088 | 24.6 | 0.790 | 21.321 | 37.8 | 53.1 |
| 8 | 450 | 6.0 | 0.909 | 23.1 | 0.580 | 16.081 | 50.1 | 35.6 |
| 9 | 450 | 8.0 | 1.048 | 24.3 | 0.779 | 22.451 | 35.9 | 56.7 |
| 11 | 450 | 4.0 | 1.121 | 24.0 | 0.800 | 20.257 | 39.8 | 49.2 |
| 13 | 450 | 6.2 | 1.162 | 24.0 | 0.900 | 23.613 | 34.1 | 65.1 |
| 14 | 450 | 4.0 | 1.143 | 23.9 | 0.795 | 23.266 | 34.7 | 45.5 |
| Geometric Mean | | 5.9 | 1.230 | 23.7 | 0.881 | 22.786 | 41.2 | 59.9 |
| Arithmetic Mean | | 6.1 | 1.279 | 23.7 | 0.936 | 23.652 | 42.5 | 79.7 |
| SD | | 1.6 | 0.418 | 0.8 | 0.420 | 7.907 | 11.4 | 75.8 |
| CV% | | 26.2 | 32.7 | 3.5 | 44.9 | 33.4 | 26.8 | 95.1 |
| Unbound Ceritinib | | | | | | | | |
| Patient# | | T _{ss,max} (h) | C _{ss,max} (μmol/L) | T _{ss,min} (h) | C _{ss,min} (μmol/L) | AUC _τ (μmol/L·h) | AUC _u /AUC _t | |
| 1 | | 8.1 | 0.042 | 24.0 | 0.020 | 0.602 | 0.013 | |
| 2 | | 6.0 | 0.021 | 24.0 | 0.014 | 0.335 | 0.017 | |
| 3 | | 6.0 | 0.025 | 24.1 | 0.014 | 0.360 | 0.015 | |
| 5 | | 21.6 | 0.010 | 21.6 | 0.010 | 0.190 | 0.010 | |
| 7 | | 24.6 | 0.011 | 24.6 | 0.011 | 0.175 | 0.008 | |
| 8 | | 6.0 | 0.015 | 23.1 | 0.011 | 0.263 | 0.016 | |
| 9 | | 1.0 | 0.002 | 24.3 | 0.001 | 0.020 | 0.001 | |
| 11 | | 6.0 | 0.017 | 24.0 | 0.011 | 0.265 | 0.013 | |
| 13 | | 6.2 | 0.024 | 24.0 | 0.014 | 0.364 | 0.015 | |
| 14 | | 7.9 | 0.025 | 23.9 | 0.018 | 0.500 | 0.022 | |
| Geometric Mean | | 7.0 | 0.015 | 23.7 | 0.010 | 0.239 | 0.010 | |
| Arithmetic Mean | | 9.3 | 0.019 | 23.7 | 0.012 | 0.307 | 0.013 | |
| SD | | 7.5 | 0.011 | 0.8 | 0.005 | 0.166 | 0.006 | |
| CV% | | 80.5 | 57.2 | 3.5 | 42.4 | 54.1 | 43.5 | |

Plasma pharmacokinetic parameters were estimated using the non-compartmental analysis.

Abbreviations: C_{ss,max}, steady-state peak plasma concentration; T_{ss,max}, time to reach the C_{ss,max}; C_{ss,min}, steady-state trough plasma concentration; T_{ss,min}, trough sampling time; AUC_τ, steady-state area under the plasma concentration – time curve during one dosing interval; CL/F, apparent clearance for the total drug; T_{1/2}, elimination half-life; AUC_u/AUC_t, unbound-to-total drug AUC ratio.

Table 3. The concentrations of total and unbound ceritinib in enhancing, non-enhancing brain tumors, and CSF, as well as the extent of penetration (K_p and $K_{p,uu}$) in patients

| Pat# | Time | Total drug tumor conc. (nmol/mg) | | Unbound drug tumor conc. (nmol/mg) | | CSF (μ M) | Fraction unbound (%) | | K_p | | $K_{p,uu}$ | |
|--------|---------|----------------------------------|--------|------------------------------------|-------|----------------|----------------------|-------|-------|-------|------------|------|
| | | EN | NE | EN | NE | | EN | NE | EN | NE | EN | NE |
| 001 | 2-4 h | 53.775 | NA | 0.870 | NA | 0.103 | 1.618 | NA | 30.43 | NA | 40.64 | NA |
| 002 | 2-4 h | 13.275 | NA | 0.005 | NA | 0.001 | 0.039 | NA | 14.22 | NA | 0.34 | NA |
| 003 | 2-4 h | 139.425 | NA | 0.065 | NA | 0.008 | 0.047 | NA | 68.88 | NA | 2.17 | NA |
| 005 | 2-4 h | 93.836 | 36.351 | 0.053 | 0.017 | 0.009 | 0.056 | 0.045 | 95.86 | 37.14 | 4.11 | 1.29 |
| 011 | 2-4 h | 2.023 | 1.259 | BLQ | BLQ | 0.017 | 0.003 | 0.006 | 2.49 | 1.55 | 0.01 | 0.01 |
| 007 | 6-8 h | 58.893 | 1.741 | 0.018 | 0.001 | 0.015 | 0.030 | 0.030 | 64.25 | 1.90 | 1.55 | 0.05 |
| 009 | 6-8 h | 17.770 | 1.490 | 0.001 | BLQ | NA | 0.006 | 0.006 | 22.90 | 1.92 | 1.32 | 0.11 |
| 013 | 6-8 h | 28.484 | 16.263 | 0.043 | 0.027 | 0.003 | 0.153 | 0.163 | 34.66 | 19.79 | 4.43 | 2.71 |
| 008 | 23-25 h | 18.340 | 7.840 | 0.055 | 0.007 | NA | 0.298 | 0.090 | 31.62 | 13.52 | 4.99 | 0.65 |
| 014 | 23-25 h | 43.715 | 2.771 | 0.063 | 0.006 | 0.015 | 0.144 | 0.213 | 54.99 | 3.49 | 3.54 | 0.33 |
| Median | | 36.100 | 2.771 | 0.048 | 0.006 | 0.012 | 0.051 | 0.045 | 33.14 | 3.49 | 2.86 | 0.33 |
| Mean | | 46.954 | 9.674 | 0.117 | 0.008 | 0.022 | 0.239 | 0.079 | 42.03 | 11.33 | 6.31 | 0.73 |
| SD | | 42.312 | 12.954 | 0.266 | 0.010 | 0.034 | 0.493 | 0.081 | 28.44 | 13.40 | 12.19 | 0.98 |
| CV% | | 90 | 134 | 227 | 124 | 156 | 206 | 102 | 68 | 118 | 193 | 133 |

Abbreviations: EN, enhancing tumor; NE, non-enhancing tumor; K_p , total drug tumor-to-plasma concentration ratio; $K_{p,uu}$, unbound drug tumor-to-plasma concentration ratio; SD, standard deviation; CV, coefficient variation; NA, sample not available; BLQ, below the lower limit of quantitation

Figure Legends

Figure 1. The penetration of ceritinib into brain tumors and CSF in patients. (A) The concentrations of total ceritinib in enhancing and non-enhancing tumors. (B) The concentrations of unbound ceritinib in enhancing, non-enhancing tumors, and CSF. (C) The total drug tumor-to-plasma concentration ratio (K_p) in enhancing and non-enhancing tumors. (D) The unbound drug tumor-to-plasma concentration ratio ($K_{p,uu}$) in enhancing and non-enhancing tumors as well as unbound drug plasma-to-CSF concentration ratio. Symbols (●, ■, ▲) represent observed values, and short bars represent median values at specific time points.

Figure 2. Pharmacodynamic analyses of CNS metastases tumor tissues after ceritinib treatment. A and B. Representative IHC images and quantification of positive cells from archival and post-ceritinib treatment tumor tissue stained for pALK, pSTAT5, pJAK2, cleaved caspase 3, and phospho histone H3 staining from patients 1 and 3.

Figure 3. Pharmacodynamic analyses of glioblastoma tumor tissues after ceritinib treatment. A. Representative IHC images of archival and post-ceritinib treatment tumor tissue stained for pFAK, pIRS1, IGF1R, pIGF1R, cleaved caspase 3, and phosphor-histone H3 staining from glioblastoma patients. **B.** Quantification of percentage of positive cells in four control primary and recurrent glioblastoma tumor tissues and pre-treatment archival vs post-ceritinib treated (phase 0) tissues.

REFERENCES:

1. Ostrom QT, Gittleman H, Xu J, Kromer C, Wolinsky Y, Kruchko C, *et al.* CBTRUS Statistical Report: Primary Brain and Other Central Nervous System Tumors Diagnosed in the United States in 2009-2013. *Neuro Oncol* **2016**;18(suppl_5):v1-v75 doi 10.1093/neuonc/nov207.
2. Steeg PS. The blood-tumour barrier in cancer biology and therapy. *Nat Rev Clin Oncol* **2021** doi 10.1038/s41571-021-00529-6.
3. Kuenzi BM, Rensing Rix LL, Stewart PA, Fang B, Kinose F, Bryant AT, *et al.* Polypharmacology-based ceritinib repurposing using integrated functional proteomics. *Nat Chem Biol* **2017**;13(12):1222-31 doi 10.1038/nchembio.2489.
4. Shaw AT, Kim DW, Mehra R, Tan DS, Felip E, Chow LQ, *et al.* Ceritinib in ALK-rearranged non-small-cell lung cancer. *N Engl J Med* **2014**;370(13):1189-97 doi 10.1056/NEJMoa1311107.
5. Vewinger N, Huprich S, Seidmann L, Russo A, Alt F, Bender H, *et al.* IGF1R Is a Potential New Therapeutic Target for HGNET-BCOR Brain Tumor Patients. *Int J Mol Sci* **2019**;20(12) doi 10.3390/ijms20123027.
6. Shaw AT, Yeap BY, Mino-Kenudson M, Digumarthy SR, Costa DB, Heist RS, *et al.* Clinical features and outcome of patients with non-small-cell lung cancer who harbor EML4-ALK. *J Clin Oncol* **2009**;27(26):4247-53 doi 10.1200/JCO.2009.22.6993.
7. Rangachari D, Yamaguchi N, VanderLaan PA, Folch E, Mahadevan A, Floyd SR, *et al.* Brain metastases in patients with EGFR-mutated or ALK-rearranged non-small-cell lung cancers. *Lung Cancer* **2015**;88(1):108-11 doi 10.1016/j.lungcan.2015.01.020.
8. Lovly CM, McDonald NT, Chen H, Ortiz-Cuaran S, Heukamp LC, Yan Y, *et al.* Rationale for co-targeting IGF-1R and ALK in ALK fusion-positive lung cancer. *Nat Med* **2014**;20(9):1027-34 doi 10.1038/nm.3667.
9. Lodhia KA, Tienchaiananda P, Haluska P. Understanding the Key to Targeting the IGF Axis in Cancer: A Biomarker Assessment. *Front Oncol* **2015**;5:142 doi 10.3389/fonc.2015.00142.
10. Bondy CA, Lee WH. Patterns of insulin-like growth factor and IGF receptor gene expression in the brain. Functional implications. *Ann N Y Acad Sci* **1993**;692:33-43 doi 10.1111/j.1749-6632.1993.tb26203.x.
11. Gong Y, Ma Y, Sinyuk M, Loganathan S, Thompson RC, Sarkaria JN, *et al.* Insulin-mediated signaling promotes proliferation and survival of glioblastoma through Akt activation. *Neuro Oncol* **2016**;18(1):48-57 doi 10.1093/neuonc/nov096.
12. Saldana SM, Lee HH, Lowery FJ, Khotskaya YB, Xia W, Zhang C, *et al.* Inhibition of type I insulin-like growth factor receptor signaling attenuates the development of breast cancer brain metastasis. *PLoS One* **2013**;8(9):e73406 doi 10.1371/journal.pone.0073406.
13. Simpson A, Petnga W, Macaulay VM, Weyer-Czernilofsky U, Bogenrieder T. Insulin-Like Growth Factor (IGF) Pathway Targeting in Cancer: Role of the IGF Axis and Opportunities for Future Combination Studies. *Target Oncol* **2017**;12(5):571-97 doi 10.1007/s11523-017-0514-5.
14. Lebrun P, Baron V, Hauck CR, Schlaepfer DD, Van Obberghen E. Cell adhesion and focal adhesion kinase regulate insulin receptor substrate-1 expression. *J Biol Chem* **2000**;275(49):38371-7 doi 10.1074/jbc.M006162200.
15. Sulzmaier FJ, Jean C, Schlaepfer DD. FAK in cancer: mechanistic findings and clinical applications. *Nat Rev Cancer* **2014**;14(9):598-610 doi 10.1038/nrc3792.
16. Taliaferro-Smith L, Oberlick E, Liu T, McGlothen T, Alcaide T, Tobin R, *et al.* FAK activation is required for IGF1R-mediated regulation of EMT, migration, and invasion in mesenchymal triple negative breast cancer cells. *Oncotarget* **2015**;6(7):4757-72 doi 10.18632/oncotarget.3023.
17. Natarajan M, Hecker TP, Gladson CL. FAK signaling in anaplastic astrocytoma and glioblastoma tumors. *Cancer J* **2003**;9(2):126-33 doi 10.1097/00130404-200303000-00008.

18. Kim DW, Mehra R, Tan DSW, Felip E, Chow LQM, Camidge DR, *et al.* Activity and safety of ceritinib in patients with ALK-rearranged non-small-cell lung cancer (ASCEND-1): updated results from the multicentre, open-label, phase 1 trial. *Lancet Oncol* **2016**;17(4):452-63 doi 10.1016/S1470-2045(15)00614-2.
19. Barlesi F, KD, Bertino E.M., van den Bent M.J., Wakelee H, Wen P.Y., Garrido Lopez P., Orlov P, Majem M, McKeage M, Yu C., Hurtado F.K, Cazorla Arratia P, Song Y, Bra nle F, Shi M, Chow L.Q. Efficacy and safety of ceritinib in ALK-positive non-small cell lung cancer (NSCLC) patients with leptomeningeal metastases (LM): Results from the phase II, ASCEND-7 study. *Annals of Oncology* 2019. p v143-v58.
20. Chow LQ, F B, E.M. B, M.J. vdB, H W, P.Y. W, *et al.* Results of the ASCEND-7 phase II study evaluating ALK inhibitor (ALKi) ceritinib in patients (pts) with ALK+ non-small cell lung cancer (NSCLC) metastatic to the brain. *Annals of Oncology*. Volume 30 2019. p V602-V3.
21. Barlesi F, Garon EB, Kim DW, Felip E, Han JY, Kim JH, *et al.* Health-Related Quality of Life in KEYNOTE-010: a Phase II/III Study of Pembrolizumab Versus Docetaxel in Patients With Previously Treated Advanced, Programmed Death Ligand 1-Expressing NSCLC. *J Thorac Oncol* **2019**;14(5):793-801 doi 10.1016/j.jtho.2019.01.016.
22. Kola I, Landis J. Can the pharmaceutical industry reduce attrition rates? *Nat Rev Drug Discov* **2004**;3(8):711-5 doi 10.1038/nrd1470.
23. Kummur S, Kinders R, Rubinstein L, Parchment RE, Murgo AJ, Collins J, *et al.* Compressing drug development timelines in oncology using phase '0' trials. *Nat Rev Cancer* **2007**;7(2):131-9 doi 10.1038/nrc2066.
24. Kummur S, Rubinstein L, Kinders R, Parchment RE, Gutierrez ME, Murgo AJ, *et al.* Phase 0 clinical trials: conceptions and misconceptions. *Cancer J* **2008**;14(3):133-7 doi 10.1097/PPO.0b013e318172d6f3.
25. Vogelbaum MA, Krivosheya D, Borghei-Razavi H, Sanai N, Weller M, Wick W, *et al.* Phase 0 and window of opportunity clinical trial design in neuro-oncology: a RANO review. *Neuro Oncol* **2020**;22(11):1568-79 doi 10.1093/neuonc/noaa149.
26. Sanai N, Li J, Boerner J, Stark K, Wu J, Kim S, *et al.* Phase 0 Trial of AZD1775 in First-Recurrence Glioblastoma Patients. *Clin Cancer Res* **2018**;24(16):3820-8 doi 10.1158/1078-0432.CCR-17-3348.
27. Xu R, Shimizu F, Hovinga K, Beal K, Karimi S, Droms L, *et al.* Molecular and Clinical Effects of Notch Inhibition in Glioma Patients: A Phase 0/I Trial. *Clin Cancer Res* **2016**;22(19):4786-96 doi 10.1158/1078-0432.CCR-16-0048.
28. Bao X, Wu J, Sanai N, Li J. A liquid chromatography with tandem mass spectrometry method for quantitating total and unbound ceritinib in patient plasma and brain tumor. *J Pharm Anal* **2018**;8(1):20-6 doi 10.1016/j.jpha.2017.07.007.
29. Stupp R, Mason WP, van den Bent MJ, Weller M, Fisher B, Taphoorn MJ, *et al.* Radiotherapy plus concomitant and adjuvant temozolomide for glioblastoma. *N Engl J Med* **2005**;352(10):987-96 doi 10.1056/NEJMoa043330.
30. Cho BC, Obermannova R, Bearz A, McKeage M, Kim DW, Batra U, *et al.* Efficacy and Safety of Ceritinib (450 mg/d or 600 mg/d) With Food Versus 750-mg/d Fasted in Patients With ALK Receptor Tyrosine Kinase (ALK)-Positive NSCLC: Primary Efficacy Results From the ASCEND-8 Study. *J Thorac Oncol* **2019**;14(7):1255-65 doi 10.1016/j.jtho.2019.03.002.
31. Hong Y, Passos VQ, Huang PH, Lau YY. Population Pharmacokinetics of Ceritinib in Adult Patients With Tumors Characterized by Genetic Abnormalities in Anaplastic Lymphoma Kinase. *J Clin Pharmacol* **2017**;57(5):652-62 doi 10.1002/jcph.849.
32. Marsilje TH, Pei W, Chen B, Lu W, Uno T, Jin Y, *et al.* Synthesis, structure-activity relationships, and in vivo efficacy of the novel potent and selective anaplastic lymphoma kinase (ALK) inhibitor

- 5-chloro-N2-(2-isopropoxy-5-methyl-4-(piperidin-4-yl)phenyl)-N4-(2-(isopropylsulfonyl)phenyl)pyrimidine-2,4-diamine (LDK378) currently in phase 1 and phase 2 clinical trials. *J Med Chem* **2013**;56(14):5675-90 doi 10.1021/jm400402q.
33. Fortin D. The blood-brain barrier: its influence in the treatment of brain tumors metastases. *Curr Cancer Drug Targets* **2012**;12(3):247-59 doi 10.2174/156800912799277511.

Figure 1

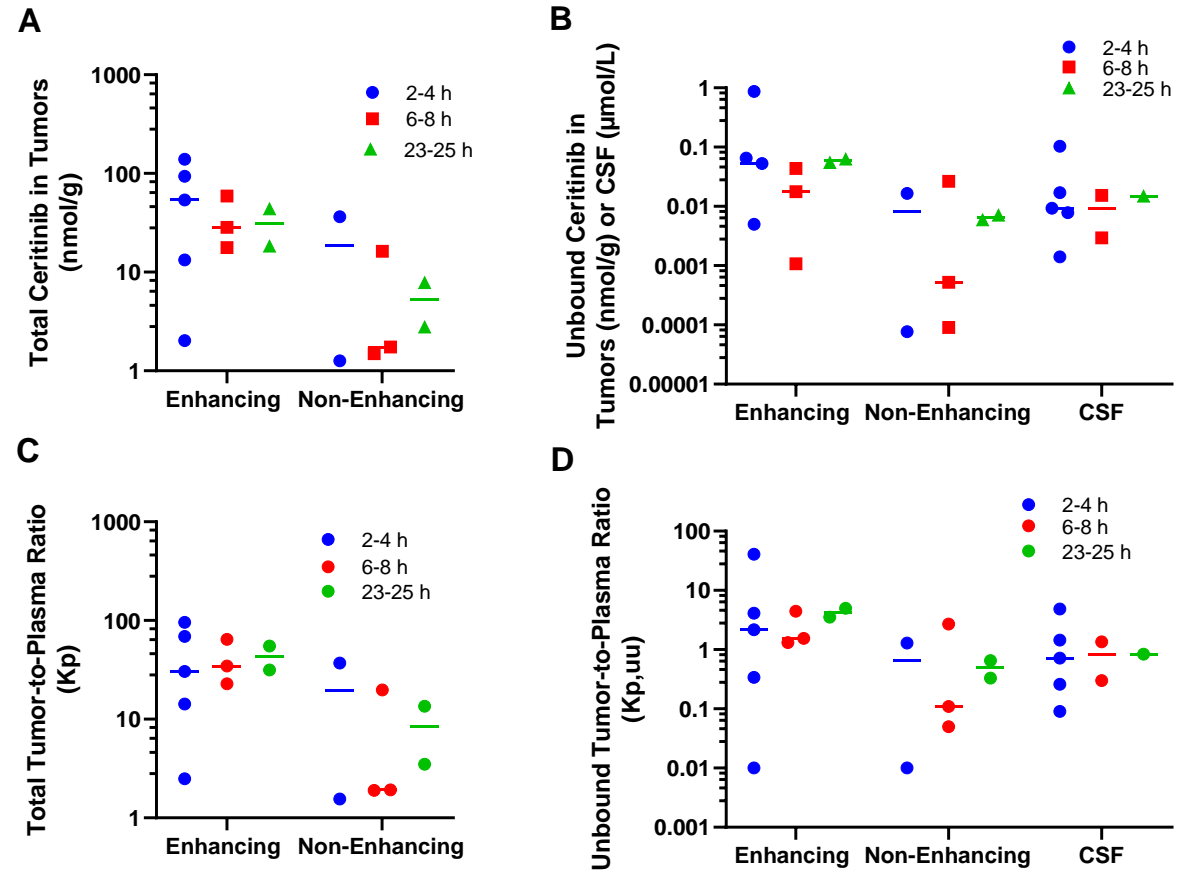


Figure 2

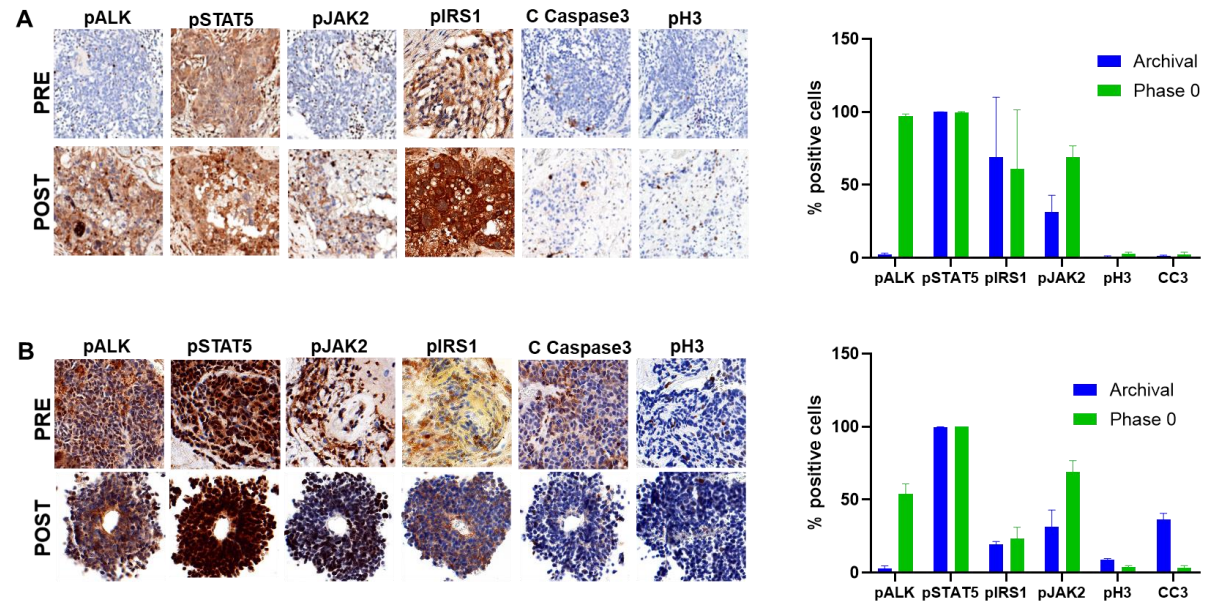
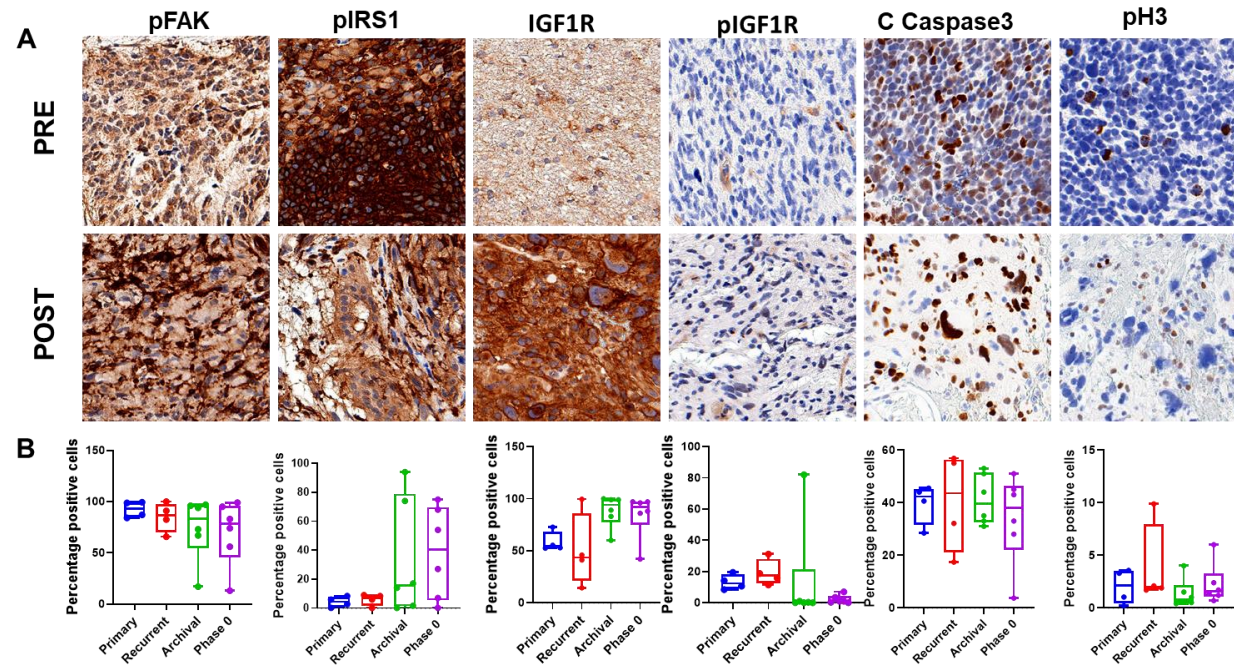


Figure 3



Clinical Cancer Research

A Phase 0 Trial of Ceritinib in Patients with Brain Metastases and Recurrent Glioblastoma

Shwetal Mehta, Roberto Fiorelli, Xun Bao, et al.

Clin Cancer Res Published OnlineFirst October 26, 2021.

Updated version Access the most recent version of this article at:
doi:[10.1158/1078-0432.CCR-21-1096](https://doi.org/10.1158/1078-0432.CCR-21-1096)

Author Manuscript Author manuscripts have been peer reviewed and accepted for publication but have not yet been edited.

E-mail alerts [Sign up to receive free email-alerts](#) related to this article or journal.

Reprints and Subscriptions To order reprints of this article or to subscribe to the journal, contact the AACR Publications Department at pubs@aacr.org.

Permissions To request permission to re-use all or part of this article, use this link <http://clincancerres.aacrjournals.org/content/early/2021/10/25/1078-0432.CCR-21-1096>. Click on "Request Permissions" which will take you to the Copyright Clearance Center's (CCC) Rightslink site.